Appl. Phys. B 74, 495–501 (2002)
DOI: 10.1007/s003400200854

Applied Physics B
Lasers and Optics

J. MORVILLE✉
D. ROMANINI

Sensitive birefringence measurement in a high-finesse resonator using diode laser optical self-locking

Laboratoire de Spectrométrie Physique, CNRS UMR 5588, Université J. Fourier, Grenoble I, B.P. 87, 38402 Saint Martin d'Hères Cedex, France

Received: 18 July 2001/Final version: 14 March 2002
Published online: 8 May 2002 •

ABSTRACT We demonstrate a new method to measure weak birefringence of dielectric mirrors with excellent spatial resolution and sensitivity ($< 10^{-7}$ radians). We exploit a well-known optical feedback scheme for line-width narrowing and frequency locking of a diode laser to a high-finesse cavity. Feedback comes from the intracavity field which builds up at resonance, selected by its change in polarization with respect to the incident field. This change, due to the residual birefringence of the cavity mirror coatings, was already exploited for birefringence measurements using an active laser-locking scheme. Here we measure the optical feedback rate as a function of rotation angle of one of the cavity mirrors (around the cavity axis). A stable feedback signal is obtained since the laser, as soon as it locks to a cavity resonance, effectively behaves as a monochromatic source. By fitting the data with a theoretical expression, we determine quantitatively the local birefringence vectors of both mirrors, which are around 10^{-6} radians. Our scheme is simple, works with cavities of very high finesse ($\mathcal{F} \sim 10^5$), and is promising for measuring birefringence in gases induced by external fields.

PACS 42.25.Lc; 42.62.Eh; 42.55.Px

1 Introduction

Optical cavities (resonator or multipass) afford a large effective interaction path in a limited physical volume, and have therefore been useful for measuring weak polarization effects [1]. Recent examples are the sensitive determination of the Verdet constant of air [2] (associated with the rotatory power induced by a magnetic field) or the Kerr constant of nitrogen, oxygen, and carbon dioxide [3] (associated with the linear birefringence induced by an electric field). More ambitious programs are devoted to the measurement of the magnetic birefringence of vacuum [4].

Some of these experiments [2–4] exploited an optical resonator (or Fabry–Pérot étalon cavity) by electronically locking the laser frequency to one of its resonances. One limitation is that the bandwidth of electronic locking is not sufficient for reducing the laser line width, which puts a limit either to the maximum cavity finesse or to the injection efficiency. In addition, when the laser line width is broader than the cavity resonance, cavity injection not only becomes less efficient but also more noisy, since the cavity converts laser frequency fluctuations (whose averaged envelope corresponds to the laser line shape) into amplitude fluctuations [5, 6].

In order to measure small polarization effects [7, 8], multipass cells have also been used. These provide a smaller path enhancement, but have the advantage of not requiring frequency locking and not being critical with respect to laser line width.

A source of error which must be considered when determining such small polarization effects is the parasitic linear birefringence $\boldsymbol{\varepsilon}$ (see exact definition below) of interferential dielectric coatings of mirrors composing cavities or multipass cells [2, 3, 7–10]. At its origin is the residual stress in the dielectric structure [2, 8]. One of the first determinations of $\boldsymbol{\varepsilon}$ realized with a multipass cell [7] produced values on the order of 10^{-4} radians per reflection, with rather negligible variations in amplitude and direction over the whole surface. In another study [9] a birefringence of a few 10^{-4} was found again, with rather small amplitude variations but with continuous directional variations of up to 40° over the mirror surface. More recently, values of $\boldsymbol{\varepsilon}$ of only a few 10^{-6} [10] or 10^{-5} [8] were measured, which perhaps indicates improving dielectric coating quality.

We present here an original measurement of the residual mirror birefringence in a stable two-mirror resonator [11]. The light field in reflection from a cavity results from the superposition of the direct input mirror reflection plus a returning fraction of the intracavity field. The intracavity component becomes important when build-up occurs at one of the cavity resonance frequencies. A polarizer followed by a Faraday rotator (which tilts the linear polarization axis by $\pi/4$), constitutes a sort of half-optical isolator. The direct reflection, which experiences a negligible polarization change, is further rotated by another $\pi/4$ on its way back; it becomes thus orthogonal to the polarizer axis and is rejected. On the other hand, the multipass effect makes the intracavity field much more sensitive to mirror birefringence, and the linear polarization of the field at the cavity input is appreciably modified. Light coming from inside the cavity is therefore partially transmit-

✉ Fax: +33-4/7651-4544, E-mail: jerome.morville@ujf-grenoble.fr

ted by the half-isolator and produces locking of the diode laser frequency to the cavity resonance, accompanied by a spectacular line-width narrowing effect to well below the cavity resonance line width [12–17]. The feedback level can be rather strong and can be observed directly, providing a means to measure intracavity birefringence effects.

We have just outlined a well-known cavity self-locking scheme based upon optical feedback, already employed for diode laser line-width narrowing and frequency stabilization [18–20]. Diode laser optical self-locking is attractive since it is robust and easy to implement. The only control parameter is the laser–cavity distance, which determines the phase of the feedback field at the laser. For phase values close to multiples of 2π, locking is stable, the cavity can be completely filled, and the feedback level is maximum. An active phase-locking mechanism would then be quite easy to implement. However, for a demonstration we simply used laser frequency sweeps in order to obtain transient locking in succession to several cavity modes. The feedback level for zero phase is then obtained without phase locking by taking the maximum feedback value over a sweep, since some of the swept modes always happen to have a feedback phase close enough to zero.

Using this scheme, important changes in the feedback level can be observed when rotating the cavity mirrors. If this is modeled by polarization matrix theory (Jones matrices), an approximate expression is found, well adapted to fit the feedback as a function of mirror rotation angle. This fit allows the determination of the mirror birefringences at the spots defined on their surfaces by the TEM_{00} mode profile (if transverse mode matching is used).

In previous experiments [2, 3] electronic frequency locking was used in order to obtain a stable and reproducible resonator transmission signal. Here, birefringence itself is exploited to obtain optical self-locking, whose superior performance resides in the dramatic laser line-width narrowing. In fact, cavities much narrower than the free-running laser line width can be used. In our demonstration, we used a diode laser with about 3-MHz FWHM line width and a cavity with mode line width close to 10 kHz.

Finally, we believe that our scheme can be used for gas-phase field-induced anisotropy measurements. We will show that the best detection limit should be obtained by rotating the mirrors to produce a minimum level of static cavity birefringence just sufficient for laser locking. In these conditions one could measure intracavity birefringence variations, induced by external field modulation, at the level of 10^{-8} radians per pass.

2 Experimental

We describe here details of our setup, following the scheme of Fig. 1. We used a distributed-feedback (DFB) multiple-quantum-well InGaAsP Mitsubishi diode laser at 1312 nm (model ML776H11F) stabilized close to room temperature to better than 0.01 K. As for all DFB diodes, this laser operates in a single mode and can be continuously tuned by temperature or current. This specific model has an excellent beam quality, with very small astigmatism and ellipticity of only 1.2. A line width of about 3 MHz was estimated by looking at the width of the high-finesse cavity resonances in

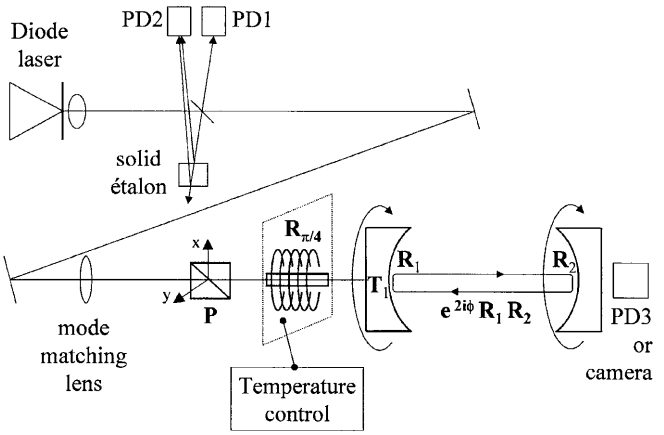

FIGURE 1 Experimental setup, with Jones matrices associated with each relevant optical component: P for the polarizer, $R_{\pi/4}$ for the Faraday rotator, and $R_{1,2}$ and $T_{1,2}$ for the mirrors' reflectivity and transmittivity, including their parasitic birefringence

transmission (adding an optical isolator temporarily). For this measurement, two stages of optical isolation (> 60 dB) were needed for unperturbed laser operation.

We used an aspheric lens (numerical aperture 0.55) to obtain a collimated beam of almost Gaussian profile. Diode laser frequency tuning by a linear current ramp was provided by a low-noise ILX current driver (model LDX3620), used in battery mode.

A beam splitter placed after the laser directed a small, calibrated, fraction of the feedback from the cavity towards a InGaAs photodiode PD1, in order to measure its intensity behavior. Additionally, a fraction of the laser beam was sent to a reference Fabry–Pérot étalon (a 3-cm-thick fused-silica uncoated flat, having a 3.45-GHz free spectral range – FSR). Fringes in reflection from this étalon were monitored by a small-area InGaAs amplified photodiode PD2. This is useful to get a picture of laser frequency tuning. A smooth sine-like signal is obtained when tuning is continuous and unperturbed. Any wanted or unwanted feedback effects were clearly visible as perturbations to this sinusoidal signal (as for the upper trace in Fig. 2).

Two mirrors where then used for alignment of the laser beam to the cavity axis. A single lens was then inserted in order to obtain preferential TEM_{00} cavity injection. Its focal length and position were determined by a mode-matching calculation taking into account the collimated laser beam diameter and other geometrical parameters of the system (cavity length, mirror curvature, laser–cavity distance, ...).

The half-isolator optics were then placed along the cavity axis, with no other element interposed before the cavity input. A CVI-Laser (CPAS-8) uncoated calcite polarizer, with a specified extinction ratio of 2×10^{-6}, was aligned with the polarization axis of the laser (vertical). The Faraday rotator was an antireflection-coated yttrium iron garnet (YIG) crystal (Isowave), of thickness 2.15 mm, adapted for a $\pi/4$ rotation at 1310 nm. It was placed inside a toroïdal permanent magnet saturating the Faraday effect in the crystal (for better homogeneity). The temperature of this Faraday assembly was controlled and used for fine tuning the rotation to exactly $\pi/4$, and thus to optimize the isolation from the direct cavity input-mirror reflection. This was the main source of

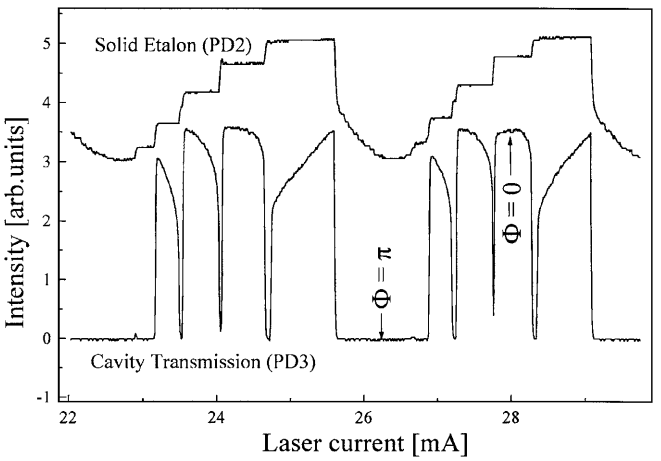

FIGURE 2 Cavity transmission showing transient optical locking to TEM_{00} resonances (*flat sections* in the *upper reference Fabry–Perot trace*) as the diode laser is frequency-tuned. The feedback phase Φ oscillates with a period depending on the laser–cavity distance. As this is not a multiple of the cavity length, the feedback for a sequence of modes goes in- and out of phase (roughly two beating periods occur in this laser scan). Since cavity resonances correspond to different values of Φ, locking gives different transmission patterns (*lower trace*). When Φ is close to zero, the mode transmission profile reaches a maximum value where the (feedback-narrowed) laser line goes exactly through the center of the cavity resonance, giving the maximum of the cavity transmission function

parasitic feedback, which was monitored by the small horizontal steps it produced on the sinusoidal reference étalon response. These steps, corresponding to constant-frequency regions, were indeed spaced by a FSR corresponding to the laser–cavity distance. No other sources of laser frequency perturbation were noticed. The Faraday isolator was optimized by reducing the size of these steps. These could never be completely eliminated, and a direct measure of the corresponding feedback rate gave about 10^{-5} at minimum.

Each cavity mirror was mounted on a tilt stage, itself attached to a rotation stage, itself fixed onto another tilt stage. Together with the incoming beam alignment, this gave enough degrees of freedom for aligning the system so that each mirror could be rotated without losing cavity injection. When the output mirror was rotated, only minor cavity adjustments were needed in order to return to TEM_{00} excitation. However, rotation of the input mirror produced a small walk-off of the transmitted incoming beam, due to a small mirror wedge. This required more important realignment of both mirrors.

Mode matching could be optimized by imaging directly the cavity output onto the sensitive surface of an infrared camera (Hamamatsu VIDICON). Excitation of different transverse modes in succession could be visualized while slowly tuning the laser frequency. When alignment was optimum, almost only TEM_{00} modes could be seen. It is to be noted that optical locking enhances mode-selective cavity excitation: when the transverse coupling of the laser beam with a given transverse mode drops below a certain value, optical feedback becomes insufficient for locking and injection of that mode becomes practically negligible.

The cavity dielectric mirrors, of 1-m radius, were coated for 1300 nm by Research Electro Optics. A third fast (1 MHz) InGaAs photodiode PD3 was placed when needed at the cavity output. This allowed ring-down time measurements (27 μs) by just abruptly turning off the diode laser current in correspondence with an excited mode [21]. Considering the cavity length, which was set close to half the confocal length (~ 50 cm), the mirror reflection coefficient at 1312 nm was then estimated to be about 0.99994. This figure is smaller than the actual mirror reflectivity since it includes intracavity broad-band losses by air (see Sect. 5), since the cavity was not evacuated.

3 Polarization transfer matrix of a birefringent linear cavity

We will use the Jones-matrix formalism [22, 23] in order to determine the reflection transfer function of our system (cavity plus half-optical isolator), whose square absolute value gives the optical feedback rate κ. In the limit of small birefringence effects, the cavity modes are not split and this reflection transfer function resembles the isolated cavity transmission function, except that its amplitude depends on intracavity birefringence. Indeed, cavity transmission may become close to 1 if intracavity losses are small, while the polarization-selected reflection is a much smaller signal and is proportional to the intracavity 'polarization change' per pass. This is the reason why, in our birefringence measurements, we will monitor the feedback level rather than the cavity transmission. Cavity transmission will be best used to monitor cavity injection and laser self-locking behavior, as shown in Fig. 2.

We will now briefly discuss why the monochromatic response function is appropriate here, even if the free-running laser line width is much broader than the cavity resonances. From these arguments will follow that our scheme does allow precise and quantitative birefringence measurements. Resuming the theory of diode laser optical self-locking would be too long; therefore we refer to the relevant publications [12–17], and just give a very simplified physical picture.

The main point to retain is that, due to the effect of laser frequency self-locking, and the concomitant line-width narrowing, the maximum reflection rate attainable is given by the peak of the reflection transfer function. This peak value will be our observable. It is reached when the phase of the feedback field at the laser, $\Phi = \omega L_{\mathrm{LC}}/c$ (modulo 2π, with L_{LC} being the laser–cavity distance), is close to zero. This is here a simplification without consequences: in reality, due to diode laser dynamics, the maximum feedback phase has a value different from zero.

Let us therefore consider a cavity resonance whose frequency is such that $\Phi \sim 0$, and assume that the laser injection current is slowly and continuously tuned so that its frequency approaches such resonance value. As soon as some ($\sim 10^{-7}$) fraction of the laser intensity returns as a resonant feedback, the laser reacts by rapidly collapsing its line width. From this point on, the laser emission may be considered as a monochromatic wave with respect to the cavity mode line width. At the same time, the laser frequency is pulled close to the cavity resonance and its tuning speed is reduced (even as the injection current continues to sweep). The reduction

factor is close to the cavity finesse times the square root of the feedback rate. This combination of effects allows us to consider the locked laser as a slowly tuning monochromatic wave. The intracavity field has time to build up and the cavity can achieve the steady state during the passage through the resonance. Obviously, for this to be true, the free-running laser frequency tuning should already be relatively slow. The cavity monochromatic response functions (in reflection and transmission) are then well adapted to describe this adiabatic regime. Finally, as Φ is close to zero, theory shows that the locked-frequency tuning range includes the cavity resonance maximum [15], so the peak value of the cavity transfer function can be directly observed. It should be noted that the range of diode injection current for which locking to a resonance is effective ('locking range'), increases with the feedback rate.

The cavity transmission for a passage through resonance represent the self-locking process [12–17]. The cavity transmission profiles obtained as a function of laser injection current should not be expected to resemble the narrow Lorentzian-like peaks which come to mind when thinking of high-finesse cavities. In addition, when the laser tunes across several cavity resonances as in Fig. 2, the lack of congruence between the cavity length L_{cav} and laser–cavity distance L_{LC} produces a beating in the feedback phase condition. When the phase is close to zero a thick and rounded frequency-locked transmission profile is observed. When $\Phi \sim \pi$ no locking occurs and cavity modes seem to be missing altogether. For intermediate phase values the transmission profile is asymmetric and does not reach the maximum of the cavity transmission function. Finally, as we explained above, close to zero-phase conditions the maximum of these transmission profiles gives directly the peak value of the cavity transmission function. It is as if a magnifying lens was used to look at the very narrow tip of the cavity resonance. The same holds for the feedback level (observed in reflection) which is, as we already pointed out, very sensitive to intracavity birefringence effects.

We will assume that the laser beam is perfectly mode-matched and only TEM_{00} resonances are excited. Naming for the Jones matrices associated with relevant optical elements is defined in Fig. 1. We reproduce here the derivation by Vallet et al. [2], adapted to our specific problem. The reflected cavity field can be written as a sum over all multiple-reflection paths, accounting for the number of transmissions and reflections for each path. Neglecting at once, for the reasons given above, the direct reflection input mirror contribution, we can write the matrix for the reflection cavity response as

$$\boldsymbol{M}_R = \boldsymbol{T}_1 \left(\sum_{n=0}^{\infty} \left[\mathrm{e}^{2\mathrm{i}\phi} \boldsymbol{R}_2 \boldsymbol{R}_1 \right]^n \right) \boldsymbol{R}_2 \boldsymbol{T}_1 \mathrm{e}^{2\mathrm{i}\phi} , \tag{1}$$

where $\phi = \omega L_{\mathrm{cav}}/c$ is the phase accumulated over one cavity length. The matrix $\boldsymbol{T}_1$ corresponds to the input mirror transmission, including its substrate birefringence. Thus this is a Jones matrix which multiplies the field transmission coefficient t_1 of the mirror. Matrices $\boldsymbol{R}_{1,2}$ are given by $\boldsymbol{R}_{1,2} = r_{1,2}\boldsymbol{M}_{1,2}$, where $r_{1,2}$ are the field reflection coefficients of the input and output mirrors, and $\boldsymbol{M}_{1,2}$ are the Jones matrices [22] for the linear birefringence $\boldsymbol{\varepsilon}_{1,2}$ of each mirror:

$$\boldsymbol{M}_{1,2} = \begin{pmatrix} A_{1,2} & B_{1,2} \\ B_{1,2} & \overline{A}_{1,2} \end{pmatrix}, \quad \text{with:}$$

$$A_{1,2} = \cos\left(\frac{\varepsilon_{1,2}}{2}\right) + \mathrm{i}\cos(2\theta_{1,2}) \sin\left(\frac{\varepsilon_{1,2}}{2}\right) ,$$

$$B_{1,2} = \mathrm{i}\sin(2\theta_{1,2}) \sin\left(\frac{\varepsilon_{1,2}}{2}\right) , \tag{2}$$

where $\varepsilon_{1,2}$ is the modulus of $\boldsymbol{\varepsilon}_{1,2}$ (defined as the phase difference for linearly polarized light coming along the slow and fast axes of the birefringent element), and $\theta_{1,2}$ its angle with the x axis (the birefringence vector points along the slow axis). In order to calculate the geometric sum it is standard procedure to use diagonalization. Indeed, if $\boldsymbol{V}$ is the matrix having the eigenvectors of $(\boldsymbol{M}_2\boldsymbol{M}_1)$ as columns, and $\boldsymbol{\Lambda}$ the diagonal matrix of the corresponding eigenvalues (here complex conjugates), one can also write

$$\boldsymbol{V}^{-1}(\boldsymbol{M}_2\boldsymbol{M}_1)^n\boldsymbol{V} = \boldsymbol{\Lambda}^n = \begin{pmatrix} \lambda^n & 0 \\ 0 & \overline{\lambda}^n \end{pmatrix}, \tag{3}$$

which allows the calculation of the geometric sum directly over the eigenvalues. In terms of the m_{ij} elements of the $(\boldsymbol{M}_2\boldsymbol{M}_1)$ matrix, the eigenvalues are obtained directly as

$$\{\lambda, \overline{\lambda}\} = \frac{1}{2}\left(m_{00} + m_{11} \pm \sqrt{(m_{00}-m_{11})^2 + 4m_{01}m_{10}} \right) . \tag{4}$$

If we now add the polarizer and Faraday rotator, which eliminate most of the direct input mirror reflection (already excluded in (1)), the matrix for the intracavity field component giving feedback to the laser is

$$\boldsymbol{M}_{\mathrm{FB}} = \boldsymbol{P}\boldsymbol{R}_{\pi/4}\boldsymbol{M}_R\boldsymbol{R}_{\pi/4}\boldsymbol{P} , \tag{5}$$

where the polarizer is oriented along the (vertical) x axis:

$$\boldsymbol{P} = \begin{pmatrix} 1 & 0 \\ 0 & 0 \end{pmatrix} , \tag{6}$$

and the Faraday $\pi/4$ rotator is given simply by a rotation matrix

$$\boldsymbol{R}_{\pi/4} = \frac{1}{\sqrt{2}} \begin{pmatrix} 1 & -1 \\ 1 & 1 \end{pmatrix} . \tag{7}$$

Substrate birefringence, induced mostly by mechanical stress, may be larger than that of the dielectric coating, but the latter is amplified by the intracavity effect. Even if substrate effects should be taken into account for a correct evaluation of the sensitivity, they can be neglected (by replacing $\boldsymbol{T}_1$ with t_1) if we want to evaluate the feedback rate. By the same argument, we will also replace with r_2 the lonely $\boldsymbol{R}_2$ matrix appearing outside the geometric sum in (1).

With these simplifying assumptions, one obtains

$$\boldsymbol{M}_{\mathrm{FB}} = \frac{1}{2} \frac{t_1^2 r_2 \mathrm{e}^{2\mathrm{i}\phi}}{(1-\lambda r_1 r_2 \mathrm{e}^{2\mathrm{i}\phi})(1-\overline{\lambda} r_1 r_2 \mathrm{e}^{\mathrm{i}2\phi})} (m_{11} - m_{00} + m_{10} - m_{01}) \begin{pmatrix} 1 & 0 \\ 0 & 0 \end{pmatrix} . \tag{8}$$

The fraction of the laser intensity coming as feedback, which we define as the coupling rate $\kappa = I_{\mathrm{FB}}(\omega)/I_{\mathrm{laser}}(\omega)$, is given by the square absolute value of $\boldsymbol{M}_{\mathrm{FB}}$. Let us consider mirrors of the same reflectivity, and introduce their reflection, transmission, and loss coefficients for the intensity (then, $\mathcal{R} = |r_{1,2}|^2$ and $\mathcal{T} = |t_{1,2}|^2$), which are constrained by energy conservation as $\mathcal{R} + \mathcal{T} + \mathcal{L} = 1$. The coupling rate is then

$$\kappa = \frac{\mathcal{F}^2\mathcal{R}^2}{2\pi^2} H_{\max} \times \frac{|m_{11} - m_{00} + m_{10} - m_{01}|^2}{\left[1 + 4\left(\frac{\mathcal{F}^2}{\pi^2}\right)\sin^2(\phi + \arg(\lambda)/2)\right]\left[1 + 4\left(\frac{\mathcal{F}^2}{\pi^2}\right)\sin^2(\phi - \arg(\lambda)/2)\right]}, \tag{9}$$

where $\mathcal{F} = \pi\sqrt{\mathcal{R}}/(1-\mathcal{R})$ is the cavity finesse, and $H_{\max} = \mathcal{T}^2/(1-\mathcal{R})^2$ takes into account mirror losses, which limit maximum intracavity buildup when the stationary state at resonance is reached. We note that information relative to mirror birefringence is contained in the eigenvalues $\lambda, \overline{\lambda}$ and in the matrix elements m_{ij}. The two resonance terms in the denominator correspond to the polarization modes which are split by the intracavity birefringence. However, as long as their separation is smaller than the width of cavity resonances ($\arg(\lambda) < 2\pi/\mathcal{F}$), these polarization modes will not be distinguishable and the laser will lock-to and inject both at the same time.

As birefringence is always much smaller than 1, we can use a first-order expansion in ε_1 and ε_2 for the matrix elements of $\boldsymbol{M}_{1,2}$ in (2) and for the eigenvalues in (4). This expansion lends an explicit analytic expression for (9), which is already rather simple. However, the denominator turns out to have only zero-order terms and ε^2 terms, and no first-order terms. This implies that the polarization modes rapidly converge to the same frequency for small ε's. Indeed, even with the high finesse of our cavity, we find that for typical birefringence values ($< 10^{-5}$) the mode splitting is much smaller than the mode width. We can therefore neglect the second-order terms in the denominator and obtain an even simpler approximate expression:

$$\kappa = \frac{\mathcal{F}^2\mathcal{R}^2}{4\pi^2} H_{\max} \left(\frac{\varepsilon_1 \cos 2\theta_1 + \varepsilon_2 \cos 2\theta_2}{1 + 4\left(\frac{\mathcal{F}^2}{\pi^2}\right)\sin^2\phi}\right)^2. \tag{10}$$

This expression gives some physical insight, and will also be used for fitting the observed feedback rate profiles obtained as a function of mirror rotation. Maximum feedback is observed when the slow axes of the mirrors are both aligned with the polarizer (x axis). The polarization eigenstates of the cavity are in this case linear, and their phase difference turns out to be maximum and equal to $\varepsilon_1 + \varepsilon_2$. The laser beam polarization, tilted at $\pi/4$ after the Faraday rotator, decomposes in equal proportions on the cavity eigenstates. The phase difference which increases with the multiple round trips inside the cavity gives then a non-zero projection of these two components when they are recombined by the polarizer on their way back to the laser. On the other hand, when the birefringence axes of the two mirrors are at $\pi/4$ or $3\pi/4$ the polarization eigenvectors are still linear, but aligned with the Faraday output. Only one eigenvector is excited, no intracavity polarization change is produced, and no locking is observed (minima in Fig. 3).

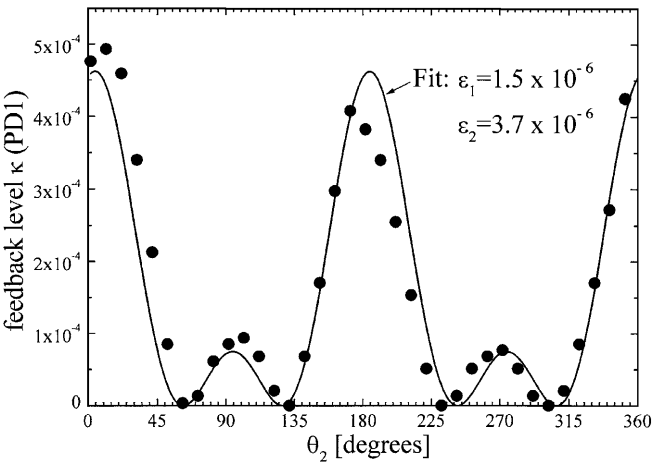

FIGURE 3 Evaluation of birefringence $\boldsymbol{\varepsilon}_1, \boldsymbol{\varepsilon}_2$ for cavity input and output mirrors by a fit (*continuous line*) of data (*black dots*) using the model derived here (10). The slow axis of the input mirror was first oriented parallel to the polarizer axis (note that the output mirror was also arbitrarily oriented close to a maximum for $\theta_2 = 0$)

Finally, we note the important enhancement of the intracavity birefringence by a factor proportional to the square of the finesse. For our cavity this factor amounts to about $(50\,900/2\pi)^2 \simeq 6.6 \times 10^7$. This property is crucial for high-sensitivity measurements, as was perhaps first discussed by Vallet et al. [2], who also introduced the name 'Malus Fabry–Pérot interferometer' for a system where a high-finesse cavity is placed between crossed polarizers. It can be understood by considering that the number of effective cavity passes (before 1/e intensity attenuation) is $\sim \mathcal{F}/\pi$. The dephasing accumulated by the circulating intracavity field is then proportional to $\mathcal{F}/\pi$ times ε (net dephasing per pass due to intracavity birefringence). The cavity output projected by a crossed polarizer is then simply proportional to $\varepsilon\mathcal{F}/\pi$ (if this is still a small dephasing). The square comes when detecting the intensity rather than the field.

It is interesting to consider what happens for large intracavity birefringence. At some point the polarization mode splitting becomes important with respect to the mode width, and second-order terms in the denominator of (9) must be considered. Numerical evaluation of the feedback rate as a function of frequency shows two distinct peaks of equal intensity. Further augmentation of ε does not increase the intensity of these peaks but only their separation. In this limit, optical feedback to the laser becomes more complicated to describe and our scheme would probably stop working.

4 Mirror birefringence measurements

Measurements were based on the determination of the feedback level, a fraction of which was detected directly using a beam splitter and a photodiode (PD1 in Fig. 1). Rather than trying to keep the laser frequency on a cavity resonance, which could also be done by controlling L_{LC} (laser–cavity separation), we modulated the laser injection current by a linear ramp to have its frequency sweeping through several cavity resonances. The laser would then lock to those resonances

with wavelengths corresponding to feedback phase close to zero. This condition occurs periodically every N resonances, with N depending upon the ratio of L_{cav} and L_{LC}. In our case, as can be seen in Fig. 2, this period was rather small, so that a small laser sweep was needed to determine the maximum of the feedback signal for each mirror configuration. We stress again that the maximum of the observed signal, for a mode with phase close to zero, depends only on the cavity, and not on the laser locking details, as long as we are in the adiabatic locking regime [12–17] that is accessible for a sufficiently slow laser tuning speed. In this limit, the laser narrowing time and the cavity buildup time are shorter than time during which locking to the resonance occurs (flat regions on the reference étalon trace in Fig. 2). Since the laser line width becomes much narrower than the cavity resonance, efficient and stable injection is obtained at the passage through resonance. The maximum of the transmission or feedback response functions can thus be easily determined to be about 1% without the need for averaging.

As expected from (10), by rotating any of the cavity mirrors around the cavity axis, an oscillatory behavior of the feedback intensity was observed. Due to the input mirror wedge, rotating this mirror induced important walk-off in the cavity injection axis. In particular the reflection spot on the output mirror would move appreciably, with associated changes of local surface birefringence. The feedback profiles obtained were substantially distorted by this effect. On the other hand, after setting the input mirror to a feedback maximum ($\theta_1 = 0$ or $\pi/2$), we recorded the feedback as a function of output mirror rotation. In this case only minor adjustments were needed every few mirror rotation steps, mostly attributed to mechanical imperfection in the alignment system.

In Fig. 3 we plot the feedback rate κ (measured at photodiode PD1) for different values of the output mirror angle θ_2. A non-linear fit by (10) is very satisfactory, as can be seen in the same figure. For this fit a value of $H_{max} = 0.24$ (accurate to a few % was used, as obtained from the cavity peak transmission normalized by intensity at the cavity input. A finesse value of $\mathcal{F} = 50\,900 \pm 1\%$ was obtained from the measurement of the cavity ring-down time ($\tau_{rd} = 27\,\mu s \pm 1\%$). The value of θ_1 was set to 0, since the input mirror was rotated to a local feedback maximum. Also, in (10), θ_2 was replaced by $\theta_2 - \Delta\theta_2$, to allow introducing an additional fit parameter (besides $\varepsilon_{1,2}$) accounting for the zero of the output mirror birefringence angle. Indeed, the orientation of the anisotropy of this mirror was not known beforehand. We obtain $\varepsilon_1 = 1.5 \times 10^{-6} \pm 5\%$ for the input mirror and $\varepsilon_2 = 3.7 \times 10^{-6} \pm 10\%$ for the output mirror, where error bars are obtained from the fitting procedure (and $\Delta\theta_2 = 4.3°$). These are values close to those previously observed by other authors for similar high-quality dielectric mirrors [10].

Small deviations of data points from the fit curve appear to be systematic rather than due to random noise. We think that the observed profile distortion is due to a residual small displacement of the mirror surface with respect to the cavity axis during rotation. This induces small variations in the local birefringence value, but also a change of the degree of transverse mode matching. Indeed, if the projection of the laser beam onto the cavity TEM_{00} mode decreases after mirror rotation, the cavity injection and thus the feedback rate also decrease. Such artifacts, which affected the accuracy of our results, were thus due to imperfection in our mechanics, which could be substantially improved. On the other hand, for intracavity measurement of gas-phase birefringence effects, discussed in Sect. 5, mirror rotation would not be needed.

5 Conclusions: Birefringence measurement perspectives and sensitivity considerations

In this paper we have proposed a new method for small birefringence measurement, and demonstrated its feasibility. Improvements are possible and measurements should be performed which could be compared with known literature values from other techniques. For this, we plan gas-phase measurements of Verdet or Kerr effects, whose coefficients are well known.

In fact, our scheme can be applied directly to determine any intracavity source of linear birefringence, such as in the case of the Kerr effect in a gas [3]. The gas birefringence induced by an electric field would appear as a $\varepsilon_K \cos(2\theta_K)$ term added to the other two similar terms in the numerator of (10). In order to differentiate it from the effect of the mirrors, the simplest solution would be to modulate the external field amplitude or direction at a slower rate than used for the laser frequency scans needed to obtain the cavity feedback rate. This would allow us to measure the corresponding feedback variations.

Alternatively, the laser–cavity distance could be controlled (e.g. using a piezoelectrically mounted mirror), and static optical locking could be achieved (without laser tuning) by a (slow) electronic servo-loop maintaining an optical feedback phase close to 0. A faster external field modulation could then be used together with sensitive lock-in detection.

Measurement of circular birefringences could also be addressed, for example as for the Verdet constant of gases [2]. The appropriate model for the feedback dependence for this case is easy to obtain by the same mathematical procedure outlined above.

Other schemes should be explored which also rely on intracavity polarization changes as a means of selecting the intracavity field for optical feedback. For example, a known scheme is using a polarizer followed by a quarter-wave plate, which has similar performance to our Faraday half-isolator. This would produce a circular rather than a linear polarization at the cavity input, making the feedback rate a function of just $\theta_1 - \theta_2$.

With respect to the sensitivity, we begin by noticing that the $\mathcal{F}^2$ enhancement of the intracavity birefringence implies that detecting smaller polarization effects is possible by using higher-finesse cavities. Contrary to previous schemes based on active brute-force electronic locking, our scheme should keep working well even with cavities of even higher finesse than used here.

The minimum feedback rate needed for diode laser optical locking is on the order of 10^{-6}. Lower levels do not give stable locking, as frequency and thus amplitude fluctuations in the cavity injection become important. In addition, a practical limit is parasitic feedback, for example from the residual input mirror reflection. It seems difficult to reduce this to much less

than 10^{-5}, due to limitation of optical components in the half-isolator arrangement, but especially due to induced or residual mirror substrate birefringence [24, 25].

From (10) we see that $\kappa \propto \varepsilon^2$, where we use $\varepsilon = \varepsilon_1 \cos 2\theta_1 + \varepsilon_2 \cos 2\theta_2$. We see therefore that

$$\frac{\delta\kappa}{\kappa} = 2\frac{\delta\varepsilon}{\varepsilon}. \tag{11}$$

Thus, if we detect 1% feedback rate variations (rather easy), we are sensitive to intracavity birefringence amplitude variations of 0.5% with respect to the total mirror birefringence ε. By rotating the mirrors we then tune this reference level down to the minimum needed for stable optical feedback. With our setup, $\varepsilon = 10^{-6}$ gives about 5×10^{-5} feedback, which is more than adequate. We could therefore detect birefringence variations at least as small as 10^{-8} (radians per pass).

Systematic errors may occur in the measurement of the amplitude of the feedback rate, and in the estimation of the factor $H_{\max}$. Thus, for instance, when using (10) to fit the data, an overestimation of 10% in $H_{\max}$ will induce an underestimation of about 5% in the magnitude of both ε's. Here we obtained $H_{\max}$ by measuring the cavity intensity transmission at resonance, normalized to the incident laser intensity. It is possible to do this to 1% accuracy, but transverse mode-matching effects should be considered. Indeed, if transverse mode matching of the laser beam to the TEM_{00} cavity modes is not good enough (projection coefficient close to 1), optical feedback locking will still be efficient but not all incident energy will be coupled into TEM_{00} cavity resonances, and $H_{\max}$ will be underestimated. Another possibility is to calculate $H_{\max}$ from $\mathcal{R}$ and $\mathcal{T}$. We have seen that ring-down time measurements on the same setup give the cavity loss per round trip, which together with the cavity length allows the calculation of $\mathcal{R}$ (and $\mathcal{F}$) to better than 1% accuracy. The mirror transmission $\mathcal{T}$ can also be accurately measured by using the same laser source and exploiting the large linear dynamic range of photodiodes to directly measure the beam intensity before and after the mirror.

Finally, it is interesting to note that broadband losses in air (Rayleigh and Mie scattering), even if not negligible with respect to mirror losses, should have no consequence on our measurements. We may include these losses as part of the mirror reflectivity coefficient $\mathcal{R}$ (whose value is then effectively reduced), and all model equations remain unchanged. Indeed, the ring-down time measurement and the cavity transmission determination of $H_{\max}$ both give values which also include these scattering loss contributions.

ACKNOWLEDGEMENTS We are grateful to A. Kachanov for enlightening discussions, and to M. Chenevier for his help.

REFERENCES

1 Y.L. Grand, A.L. Floch: Opt. Lett. **17**, 360 (1992)
2 M. Vallet, F. Bretenaker, A.L. Floch, R.L. Naour, M. Oger: Opt. Commun. **168**, 423 (1999)
3 E. Inbar, A. Arie: Appl. Phys. B **70**, 849 (2000)
4 D. Bakalov, F. Brandi, G. Cantatore, G. Carugno, S. Carusotto, F. Della Valle, A.M. De Riva, U. Gastaldi, E. Iacopini, P. Micossi, E. Milotti, R. Onofrio, R. Pengo, F. Perrone, G. Petrucci, E. Polacco, C. Rizzo, G. Ruoso, E. Zavattini, G. Zavattini: Quantum Semiclass. Opt. **10**, 239 (1998)
5 A.L. Schawlow, C.H. Townes: Phys. Rev. **112**, 1940 (1958)
6 J. Morville, D. Romanini, A.A. Kachanov, M. Chenevier: submitted to Appl. Opt. LP.
7 M.A. Bouchiat, L. Pottier: Appl. Phys. B **29**, 43 (1982)
8 S. Carusotto, E. Polacco, E. Iacopini, G. Stefanini, E. Zavattini, F. Scuri: Appl. Phys. B **48**, 231 (1989)
9 P. Micossi, F.D. Valle, E. Milotti, E. Zavattini, C. Rizzo, G. Ruoso: Appl. Phys. B **57**, 95 (1993)
10 D. Jacob, M. Vallet, F. Bretenaker, A.L. Floch, M. Oger: Opt. Lett. **20**, 671 (1995)
11 A. Yariv: *Quantum Electronics*, 3rd edn. (Wiley, New York 1989)
12 H. Li, N. Abraham: IEEE J. Quantum Electron. **QE-25**, 1782 (1989)
13 R.F. Kazarinov, C.H. Henry: IEEE J. Quantum Electron. **QE-23**, 1401 (1987)
14 H. Li, H. Telle: IEEE J. Quantum Electron. **QE-25**, 257 (1989)
15 P. Laurent, A. Clairon, C. Breant: IEEE J. Quantum Electron. **QE-25**, 1131 (1989)
16 R. Lang, K. Kobayashi: IEEE J. Quantum Electron. **QE-16**, 347 (1980)
17 H. Li, N. Abraham: Appl. Phys. Lett. **53**, 2257 (1988)
18 C. Tanner, B. Masterson, C. Wieman: Opt. Lett. **13**, 357 (1988)
19 A. Hemmerich, D. McInttyre, C. Zimmermann, T. Hansch: Opt. Lett. **15**, 372 (1990)
20 R.J. Thompson, G. Rempe, H.J. Kimble: Phys. Rev. Lett. **68**, 1132 (1992)
21 D. Romanini, A. Kachanov, J. Morville, M. Chenevier: SPIE Proc. Ser. **3821**, 94 (1999)
22 S. Huard: *Polarisation de la Lumiere* (Masson, Paris 1994)
23 E. Hecht: *Optics*, 2nd edn. (Addison-Wesley, Massachusetts, 1987) Chap. 8, pp. 324–326
24 J. Poirson, T. Lanternier, J. Cotteverte, A.L. Foch, F. Bretenaker: Appl. Opt. **34**, 6806 (1995)
25 J. Poirson: Ph.D. Thesis, Université de Rennes 1, 1998